TOXICOLOGICAL SCIENCES **111(2)**, 331–344 (2009)
doi:10.1093/toxsci/kfp152
Advance Access publication July 16, 2009

Iron-Induced Oxidative Injury Differentially Regulates PI3K/Akt/GSK3β Pathway in Synaptic Endings from Adult and Aged Rats

Romina María Uranga, Norma María Giusto, and Gabriela Alejandra Salvador[1]

Instituto de Investigaciones Bioquímicas de Bahía Blanca, Universidad Nacional del Sur and Consejo Nacional de Investigaciones Científicas y Técnicas, CC 857, B8000FWB Bahía Blanca, Argentina

Received May 12, 2009; accepted July 8, 2009

In this work we study the state of phosphoinositide-3-kinase/Akt/glycogen synthase kinase 3 beta (PI3K/Akt/GSK3β) signaling during oxidative injury triggered by free iron using cerebral cortex synaptic endings isolated from adult (4-month-old) and aged (28-month-old) rats. Synaptosomes were exposed to $FeSO_4$ (50μM) for different periods of time and synaptosomal viability and the state of the PI3K/Akt/GSK3β pathway were evaluated in adult and aged animals. 3-(4,5-Dimethylthiazol-2-yl)-2,5-diphenyltetrazolium bromide reduction and lactate dehydrogenase leakage were significantly affected in both age groups. However, aged animals showed a greater susceptibility to oxidative stress. In adults, Akt was activated after a brief exposure time (5 min), whereas in aged animals activation occurred after 5 and 30 min of incubation with the metal ion. GSK3β phosphorylation showed the same activation pattern as that observed for Akt. Both Akt and GSK3β phosphorylation were dependent on PI3K activation. Extracellular signal–regulated kinases 1 and 2 (ERK1/2) activation was temporally coincident with Akt activation and was PI3K dependent in adults, whereas ERK1/2 activation in aged rats was higher than that observed in adults and showed no dependence on PI3K activity. We demonstrate here that synaptic endings from adult and aged animals subjected to iron-induced neurotoxicity show a differential profile in the activation of PI3K/Akt/GSK3β. Our results strongly suggest that the increased susceptibility of aged animals to oxidative injury provokes a differential modulation of key signaling pathways involved in synaptic plasticity and neuronal survival.

Key Words: **synaptic endings; PI3K; Akt; oxidative stress; iron; neurotoxicity.**

Transition metals—particularly iron—have been shown to contribute to Alzheimer's disease (AD) pathology and are considered responsible for generating massive oxidative damage involving lipid peroxidation and mitochondrial dysfunction (Keller *et al*., 1997; Nunomura *et al*., 2001; Zhu *et al*., 2004). Additionally, the accumulation of iron in the brain is a consistent observation in AD. In AD brains, iron accumulation occurs without ferritin increase, thereby rising the risk of oxidative stress. Metalloneurobiology has become extremely important in establishing the origin of AD and other diseases causing neuronal degeneration.

Neurons have developed several protective mechanisms against oxidative stress, among which is the activation of cellular signaling pathways. The final response will depend on the identity, intensity, and persistence of the oxidative insult. The characterization of the mechanisms mediating the effects of oxidative stress on neuronal dysfunction and death is central to understanding the pathology of a number of neurodegenerative disorders. In this context the phosphoinositide-3-kinase (PI3K) pathway has acquired particular relevance because of its pleiotropic role in cellular fate. PI3K is an enzyme that phosphorylates the 3′-OH position in the inositol ring of phosphoinositides, which are able to recruit proteins with pleckstrin homology (PH) domains to the plasma membrane. The prototype of this PH domain–containing protein is Akt (also known as PKB), which mediates PI3K action and has been associated with cell cycle progression, motility and cellular survival and proliferation (Coelho and Leevers, 2000; Fry, 2001; Katso *et al*., 2001). Activated Akt phosphorylates numerous enzymes (such as glycogen synthase kinase 3 beta, GSK3β) thus regulating a wide range of cellular functions (Datta *et al*., 1997; Kauffmann-Zeh *et al*., 1997).

Another signaling pathway closely related to PI3K is the mitogen-activated protein kinase (MAPK) pathway. The extracellular signal–regulated kinases 1 and 2 (ERK1/2) are two of the best-known components of the MAPK pathway and have been shown to be activated by oxidative stress in several biological systems (Anselmo and Cobb, 2004; Niwa *et al*., 2001; Sun *et al*., 2001; Zago *et al*., 2005). It has been suggested that together, the PI3K and MAPK pathways can play a central role in the arrangement of a cellular response to a local redox environment (Kenyon, 2005).

Synapses are held to be the sites where AD and AD-related neurodegenerative disorders are likely to begin. Abnormal synaptic signaling, accumulation of iron and an increased

[1] To whom correspondence should be addressed at Instituto de Investigaciones Bioquímicas de Bahía Blanca, Universidad Nacional del Sur and Consejo Nacional de Investigaciones Científicas y Técnicas, CC857, B8000FWB Bahía Blanca, Argentina. Fax: +54-291-4861200. E-mail: salvador@criba.edu.ar.

susceptibility to oxidative stress is thought to be the cause of this disorder. Based on the experimental support suggesting that many signaling pathways observed in intact cells can be observed in cells lacking nuclei (Jacobson *et al.*, 1994), we employed rat cortical synaptosomes, to test the hypothesis that signaling mechanisms can be activated locally in synapses. The characterization of synaptic signaling pathways during oxidative injury has attracted great interest over the last few years and we have recently demonstrated that the synaptic PI3K/Akt pathway is activated as an early oxidative stress-triggered event caused by free iron (Uranga *et al.*, 2007). However, the precise nature of the relationship between synaptic signaling downstream of Akt and oxidative stress is far from clear. The aim of this work is to study the effects of iron overload–induced oxidative stress conditions on the PI3K/Akt/GSK3β and ERK1/2 pathways in synaptic endings from both adult and aged animals.

EXPERIMENTAL PROCEDURES

Animals. Wistar-strain adult (4 months of age) and old (28 months of age) rats housed under controlled conditions (constant room temperature, 12-h light/12-h dark cycle), bred in our own colony and fed a standard rat chow diet with free access to water, were used. All the procedures were in strict accordance with the guidelines published in the *National Institutes of Health Guide for The Care and Use of Laboratory Animals*.

Materials. The kit (LDH-P UV AA) for measuring lactate dehydrogenase (LDH) activity was generously supplied by the Wiener Laboratory (Rosario, Santa Fe, Argentina). Rabbit polyclonal anti-phospho-Ser473-Akt, rabbit polyclonal anti-Akt, rabbit polyclonal anti-phospho-Ser380-PTEN, rabbit polyclonal anti-PTEN, rabbit polyclonal anti-phospho-Ser9-GSK3β, rabbit polyclonal anti-PSD95 and rabbit monoclonal anti-GSK3β were from Cell Signaling Technology (Beverly, MA). Anti-phospho-Tyr204-ERK1/2, anti-ERK2, anti-Src, polyclonal horseradish peroxidase (HRP)–conjugated goat anti-rabbit IgG, and polyclonal HRP-conjugated goat anti-mouse IgG were purchased from Santa Cruz Biotechnology, Inc. (Santa Cruz, CA). Rabbit polyclonal anti-HNE was a kind gift from Dr Koji Uchida (Laboratory of Food and Biodynamics, Graduate School of Bioagricultural Sciences, Nagoya University, Nagoya, Japan) and Dr Luke Szweda (Free Radical Biology and Aging Research Program, Oklahoma Medical Research Foundation, OK). All other reagents were of analytical grade, purchased from Sigma-Aldrich (St Louis, MO) unless stated otherwise.

Preparation of synaptosomal fraction and experimental treatments. Purified synaptosomal fraction was obtained as previously described by Cotman (1974), with slight modifications. Briefly, rats were sacrificed by decapitation, brains were removed on a cold plate, and the cerebral cortex was immediately dissected (2–4 min after decapitation) and placed in 0.32M sucrose isolation buffer containing 2 μg/ml leupeptin, 1 μg/ml pepstatin, 1 μg/ml aprotinin, 1mM dithiothreitol (DTT), 0.1mM phenylmethylsulfonyl fluoride (PMSF), 1mM EDTA, and 10mM 4-(2-hydroxyethyl)-1-piperazine ethanesulfonic acid (HEPES), pH 7.4. The cerebral cortex was homogenized by 10 strokes with a Thomas tissue homogenizer. The homogenate was then centrifuged at 1800 × g for 7.5 min at 4°C using a JA-21 rotor in a Beckman J2-21 centrifuge. The pellet was discarded, and the supernatant was retained and centrifuged at 14,000 × g for 20 min at 4°C. The resulting pellet was washed and resuspended in 3 ml of 0.32M sucrose isolation buffer and layered over a discontinuous Ficoll gradient (8.5% pH 7.4, 13% pH 7.4 Ficoll solutions, each prepared in isolation buffer) and spun at 85,500 × g for 30 min at 4°C using a SW 28.1 rotor in a Beckman L5-50 ultracentrifuge. Synaptosomes in the 8.5–13% Ficoll interface were removed, resuspended in isolation buffer, and centrifuged at 33,000 × g for 20 min at 4°C using a JA-21 rotor in a Beckman J2-21 centrifuge. Washed synaptosomal fraction was used for the experiments detailed below. Protein content of the synaptosomal fraction was determined by the method of Lowry *et al.* (1951).

Incubation of synaptosomes. Synaptosomes were diluted in Locke's buffer (154mM NaCl, 5.6mM KCl, 2.3mM $CaCl_2$, 1.0mM $MgCl_2$, 3.6mM $NaHCO_3$, 2 mg/ml glucose, 20mM HEPES, pH 7.2) for all experiments except where stated otherwise. Synaptosomal suspensions were aliquoted (2 mg protein/ml) into tubes and incubated at 37°C under an O_2:CO_2 (95:5, vol:vol) atmosphere during experimental treatments. $FeSO_4$ was prepared as a 10mM stock in water immediately prior to use.

Electron microscopy of synaptosomal preparations. Purified cerebral cortex synaptosomes obtained from adult and aged rats were fixed by ice-cold buffered (pH 7.4) isoosmotic (by the addition of sucrose) glutaraldehyde solution (end concentration 4%). The fixed synaptosomes were washed overnight with isoosmotic buffer, postosmicated, dehydrated, and flat embedded in Medcast (Ted Pella, CA) resin. Sections from four different depths of the pellets were cut on a ultramicrotone and examined in a Jeol 100 Cx II electron microscope (Coasin S.A., Buenos Aires, Argentina).

3-(4,5-Dimethylthiazol-2-yl)-2,5-diphenyltetrazolium bromide reduction assay. Neuronal viability was measured by determining cellular reducing capacity via the extent of MTT reduction to the insoluble intracellular formazan, which depends on the activity of intracellular dehydrogenases and is independent of changes in the integrity of the plasma membrane. The methods employed in the present study were similar to those described previously by Keller *et al.* (1997). In brief, MTT was dissolved in phosphate-buffered saline (PBS) at a concentration of 5 mg/ml. The MTT solution was mixed with synaptosomes (1:10 MTT:synaptosomes, vol:vol) and allowed to incubate for 2 h at 37°C. The assay was started by adding 200 μg of synaptosomal protein from adult or aged cerebral cortex to the MTT solution. At the end of incubation with MTT, solubilization buffer (20% sodium dodecyl sulfate [SDS], pH 4.7) was added and mixed thoroughly to dissolve the crystals of formazan. The extent of MTT reduction then was measured spectrophotometrically at 570 nm. Results are expressed as a percentage of control.

Measurement of LDH release. After incubation in the presence of either Fe^{2+} or vehicle, synaptosomes were centrifuged at 33,000 × g for 20 min at 4°C. The resulting supernatant was used to determine LDH activity, measured spectrophotometrically by using an LDH-P UV AA kit following the manufacturer's instructions. Briefly, the rate of conversion of reduced nicotinamide adenine dinucleotide to oxidized nicotinamide adenine dinucleotide was followed at 340 nm. Results are expressed as a percentage of the control value.

Determination of reactive oxygen species generation. Synaptosomal oxidative stress was evaluated using the probe 5 (or 6)-carboxy-2′7′-dicholorodihydrofluorecein diacetate (DCDCDHF). This probe can cross the membrane, and after oxidation, it is converted into a fluorescent compound. After the corresponding treatments, 500 μl of synaptosomal suspension (2 mg/ml) was spun down at 3,000 × g for 5 min at 4°C in a table-top microcentrifuge. The resulting synaptosomal pellet was resuspended in 500 μl of PBS containing 10μM DCDCDHF (Invitrogen, Buenos Aires, Argentina). After 30 min of incubation at 37°C synaptosomes were spun down at 3,000 × g for 5 min and resuspended in 750 μl of PBS solution. The fluorescence ($\lambda_{ex} = 538$, $\lambda_{em} = 590$) was measured in a SLM model 4800 fluorimeter (SLM Instruments, Urbana, IL). Results are expressed as a percentage of the control value.

Sodium dodecyl sulfate–polyacrylamide gel electrophoresis and Western blot assays. Samples were denatured with Laemmli sample buffer at 100°C for 5 min. Equivalent amounts of synaptosomal proteins were separated by SDS-polyacrylamide gel electrophoresis (SDS-PAGE) on 10% polyacrylamide

gels and then transferred to a polyvinylidene fluoride membrane (Millipore, Bedford, MA). Membranes were blocked with 5% nonfat dry milk in TTBS buffer (20mM Tris-HCl [pH 7.4], 100mM NaCl, and 0.1% [wt/vol] Tween 20) for 2 h at room temperature for all the Western blots assayed. Membranes were then incubated with primary antibodies (anti-phosphoSer473-Akt, anti-Akt, anti-phosphoSer9-GSK3β, anti-GSK3β, anti-phosphoSer380-PTEN, anti-PTEN, anti-phosphoTyr204-ERK1/2, anti-ERK2, anti-HNE, anti-PSD95, anti-SV2 [1:1000] overnight at 4°C), washed three times with TTBS, and then exposed to the appropriate HRP-conjugated secondary antibody (anti-rabbit or anti-mouse) for 1 h at room temperature. Membranes were again washed three times with TTBS, and immunoreactive bands were detected by enhanced chemiluminescence (ECL; GE Healthcare Bio-Sciences, Buenos Aires, Argentina) using standard X-ray film (Kodak X-OMAT AR; GE Healthcare Bio-Sciences). Several different exposure times were used for each blot to ensure linearity of band intensities. Immunoreactive bands were quantified using image analysis software (Image J, a freely available application in the public domain for image analysis and processing, developed and maintained by Wayne Rasband at the Research Services Branch, National Institute of Mental Health).

Immunoprecipitations. Src was immunoprecipitated according to Uranga *et al*. (2007). Synaptosomes (400 μg of total protein) were solubilized in NP-40 lysis buffer (20mM HEPES [pH 7.5], 1% NP-40 [wt/vol], 40mM β-glycerophosphate, 10mM ethylene glycol-bis(beta-aminoethyl ether)-N,N,N′,N′-tetra acetic acid [EGTA], 2.5mM $MgCl_2$, 0.2mM Na_3VO_4, 10mM NaF, 1mM DTT, 2 μg/ml leupeptin, 1 μg/ml aprotinin, 1 μg/ml pepstatin, 0.1mM PMSF). Insoluble material was removed by centrifugation at 17,000 × g for 20 min. The solubilized synaptosomes were precleared by mixing with 20 μl of protein A sepharose (3 mg) for 30 min and spun briefly at 500 × g. The supernatant was then incubated overnight with anti-Src antibody (10 μl/immunoprecipitate [IP]) and subsequently mixed with 50 μl of protein A sepharose (6 mg) and incubated for 4 h. All the aforementioned incubations were performed with gentle shaking at 4°C. After a short spin IPs were washed thrice with PBS, twice with 0.1M Tris-HCl (pH 7.5) buffer containing 0.5M LiCl, and twice with TNE buffer (10mM Tris-HCl [pH 7.5], 100mM NaCl, and 1mM EDTA). All wash buffers contained 0.2mM Na_3VO_4. The final IPs were resuspended in 30 μl of Laemmli sample buffer (Laemmli, 1970) for Western blot analyses.

Data analysis. Quantitative results were expressed as the mean ± SD of the *N* indicated in the corresponding figures. Data were analyzed by one-way ANOVA followed by the Tukey multiple comparison test. *p* Values less than 0.05 were considered statistically significant. Western blots shown are representative of at least three analyses performed on samples from at least three separate experiments.

RESULTS

Effect of Fe^{2+} Exposure on Synaptosomal Viability

Neurotoxic agents such as Fe^{2+} induce lipid peroxidation and impairment of glutamate and glucose transport as well as mitochondrial dysfunction. Our first goal was to characterize the effect of different concentrations of $FeSO_4$ (10, 50, and 200μM) on synaptosomal viability. To determine the effect of Fe^{2+} exposure (5, 30, and 60 min) on adult-rat cerebral cortex synaptic endings, MTT reduction was evaluated as a measure of mitochondrial function. Control conditions were also assessed, replacing Fe^{2+} by an equal volume of water (vehicle). As shown in Figure 1A, MTT reduction was significantly diminished at all the incubation times assayed in the presence of 50 and 200μM of $FeSO_4$ when compared with the corresponding controls. The lowest Fe^{2+} concentration (10μM) only affected mitochondrial viability after 60 min of exposure. Plasma membrane integrity was also evaluated by monitoring the leakage of LDH to the extrasynaptosomal medium. Figure 1B shows that Fe^{2+} induced an increase in LDH leakage at all the concentrations assayed being the greatest effect observed at 50 and 200μM concentrations. For additional characterization of the metal-induced oxidative stress model, the presence of 4-hydroxynonenal (HNE) conjugated synaptic proteins was evaluated by Western blot. Figures 1C and 1D show an increase in HNE levels as a time and concentration function.

$FeSO_4$ (50μM) was the minor concentration of iron that caused mitochondrial and membrane damage in the experimental model. Following on from this, our next objective was to characterize the effect of $FeSO_4$ (50μM) on aged-rat synaptic endings and to compare this with that observed in adult animals. As shown in Figure 2A, MTT reduction was significantly diminished at all three times of iron exposure (11, 47, and 76% lower than the corresponding controls for the 5-, 30-, and 60-min incubations, respectively). No significant differences in mitochondrial viability were observed in adult- compared with aged-rat synaptosomes after brief exposure. However, after intermediate- and long-term exposures (30 and 60 min, respectively) aged-rat synaptosomes showed a greater susceptibility to oxidative stress than that showed by synaptosomes from adult rats: MTT reduction was 27 and 52% lower in the synaptic endings from aged origin than in those from adult origin, after the incubations of 30 and 60 min, respectively. Despite the greatest susceptibility observed in aged animals, the initial state of mitochondrial activity (measured as succinate dehydrogenase specific activity) was the same than that found in adults (adult: 4.275 ± 0.129 AU/mg protein; aged 4.323 ± 0.491 AU/mg protein). Figure 2B shows that Fe^{2+} also induced a significant increase in LDH leakage in aged-rat synaptosomes after each of the three exposure periods tested (21, 133, and 148% over the control values, for the incubations of 5, 30, and 60 min, respectively). When compared with the results obtained in adult synaptosomes it can be observed that, as in the case of MTT, no significant differences were observed after a 5-min exposure. However, aged-rat synaptosomes showed greater LDH leakage compared with those of adult rats after longer exposure times (67 and 66% higher, after 30 and 60 min of incubation, respectively). Oxidative stress levels were also measured by DCDCDHF fluorescence. Reactive oxygen species (ROS) generation significantly increased at all times of incubation in the presence of Fe^{2+} with respect to the respective control. No significant differences on ROS formation were observed when compared samples from adult versus aged animals (Fig. 2C). Electron micrographs of synaptosomal preparations show synaptic endings containing intact mitochondria and no structural differences are observed between adult and aged samples (Fig. 2D). Moreover, Figure 2E shows immunoblots of two synaptic marker proteins (postsynaptic density 95 [PSD95, postsynaptic marker] and synaptic vesicle protein 2 [SV2, presynaptic marker]) in samples obtained from both age

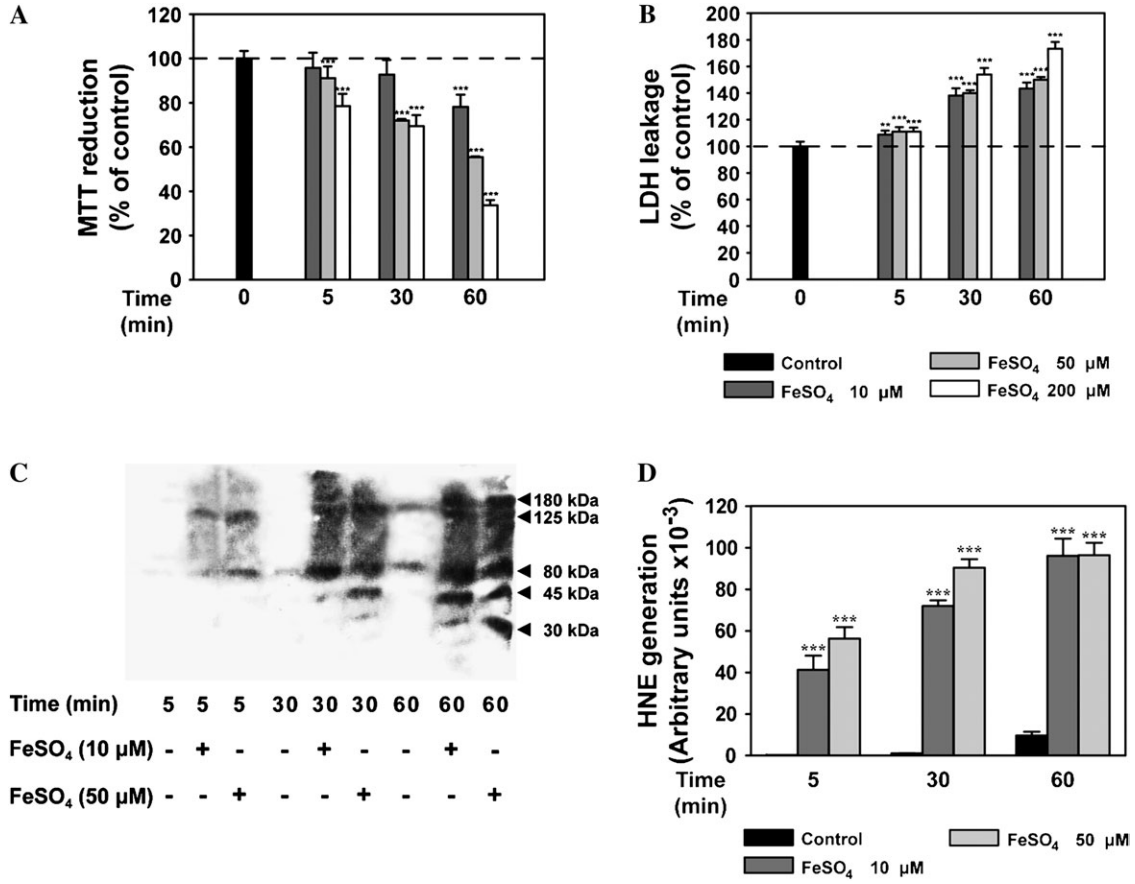

FIG. 1. Characterization of Fe^{2+}-induced damage in adult synaptosomes (2 mg protein/ml). (A) MTT reduction assay performed after 5-, 30-, and 60-min exposures to increasing Fe^{2+} concentrations (10, 50, and 200µM). $n = 3–6$. (B) Measurement of LDH release after the same incubation times and the same iron concentrations. $n = 3–6$. (C) HNE levels analyzed by Western blotting in adult synaptosomes exposed to 10 or 50µM $FeSO_4$ for 5, 30, and 60 min. Fifty micrograms of synaptosomal proteins were loaded onto 10% SDS-PAGE gels, and the blots were probed with anti-HNE antibodies (see details in the text). The Western blot is representative of three different experiments. (D) The bands of HNE shown in (C) were quantified using scanning densitometry, and the data represent the mean ± SD of three different experiments expressed in arbitrary units. ***$p < 0.001$ and **$p < 0.01$ with respect to the control condition.

groups. These results demonstrate that synaptosomal preparations had the same degree of purity when compared adult versus aged.

State of Akt and Akt-Downstream Pathways after Fe^{2+}-Induced Neurotoxicity

Figure 3A demonstrates that Fe^{2+} induced an increase in Akt phosphorylation in adult-rat synaptic endings. To test the hypothesis that Akt activation is a PI3K-dependent event, Akt phosphorylation was determined by Western blot in adult and aged-rat synaptosomes, using 10µM LY294002 (a specific PI3K inhibitor). The increase on Akt phosphorylation was inhibited when synaptosomes were incubated with LY294002 prior to incubation with the metal ion. When looking at Akt activation in aged-rat synaptosomes (Fig. 3B), we observed that Fe^{2+} activated Akt after 5 min of incubation, but also after 30 min of exposure, at which point the maximum level of activation was reached. Irrespective of the level of activation, it was in both cases PI3K dependent.

After confirming the activation of PI3K/Akt in both age groups (for comparison see Fig. 3E left panel), we decided to study GSK3β phosphorylation under the same experimental conditions. Figure 3C shows that Fe^{2+} augmented GSK3β phosphorylation in adult rats after 5 min of incubation (temporally coincident with Akt activation). The results obtained in the presence of LY294002 show that GSK3β phosphorylation is a PI3K-dependent event. GSK3β phosphorylation in aged-rat synaptosomes (Fig. 3D) augmented after 30 min of iron exposure. Preincubation with LY294002 abolished both increases in GSK3β phosphorylation, demonstrating its inhibition is also PI3K dependent in aged animals (for comparison see Fig. 3E, right panel). It is important to note that levels of Akt and GSK3β activation were significantly higher in aged animals when compared with adult ones at 30 min of incubation.

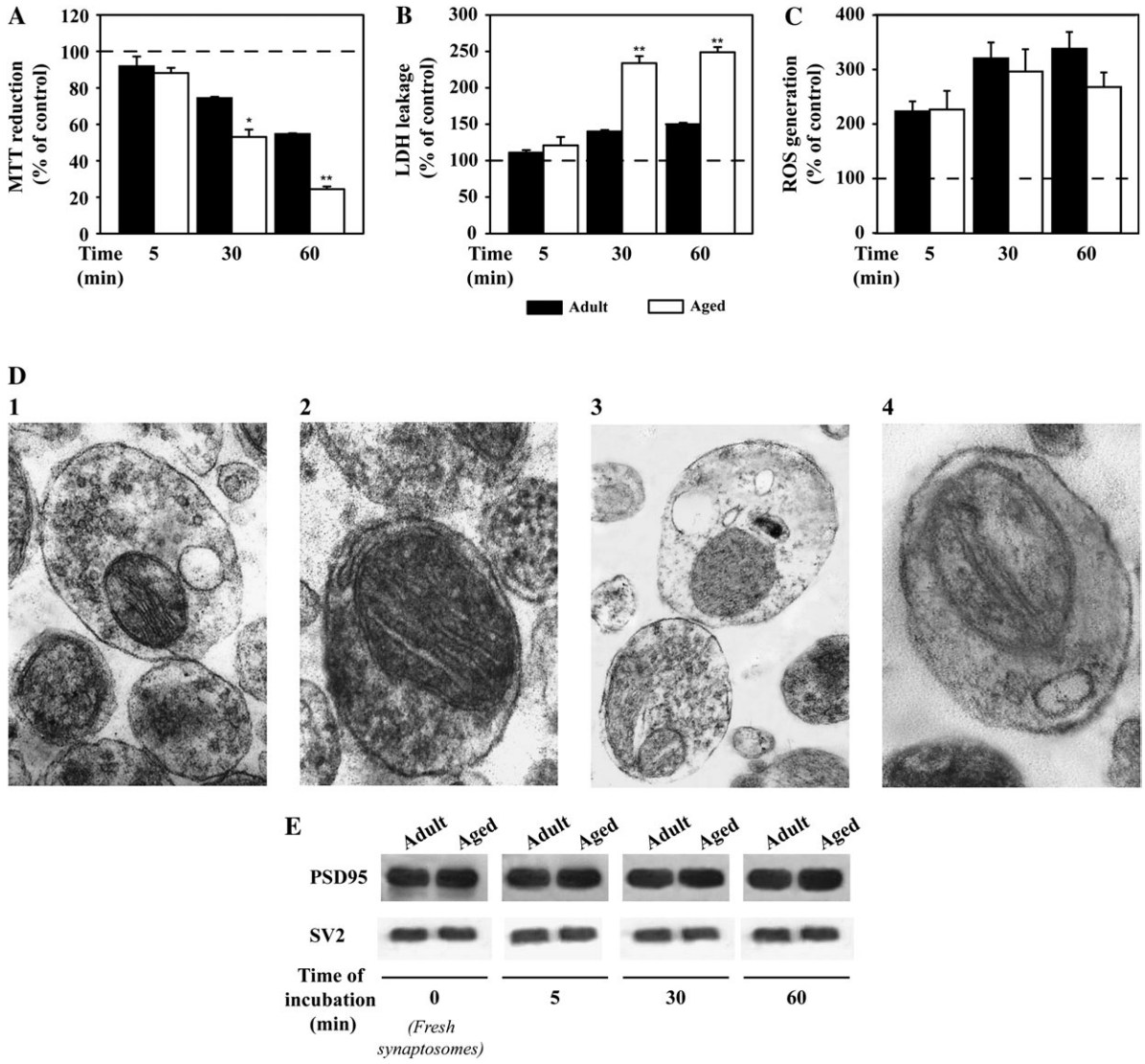

FIG. 2. Fe^{2+}-induced oxidative stress in purified rat synaptosomes. (A) MTT reduction assay performed after 5, 30, and 60 min of 50μM Fe^{2+} exposure in synaptosomes (2 mg protein/ml) from adult and aged rats. (B) Measurement of LDH release after the same incubation times in synaptosomes (2 mg protein/ml) from both age groups. (C) ROS levels were determined by the DCDCDHF fluorescence assay in synaptic endings from adult and aged rats. Results are expressed as percentage of control and represent the mean ± SD; $n = 3$–6. *$p < 0.05$ and **$p < 0.01$ versus the ''Adult'' condition studied at the same time. (D) Electron micrographs of cerebral cortex synaptosomal preparations isolated from adult (panels 1 and 2) and aged (panels 3 and 4) rats on a discontinuous Ficoll gradient. Panels 1 and 3: Medium power (×40,000) view of synaptosomal pellet. Panels 2 and 4: High power (×80,000) view of synaptosomes containing mitochondria and vesicles. (E) Western immunoblot analysis of synaptosomes for PSD95 and SV2 expression levels. Samples containing 50 μg of protein were loaded onto 10% SDS-PAGE gels, and the blots were probed with the corresponding antibodies.

Effects of Fe^{2+}-Induced Oxidative Stress on PTEN Phosphorylation

Phosphatase and tensin homolog deleted on chromosome ten (PTEN) and PI3K are known to play opposing roles in cellular signaling, so we evaluated PTEN phosphorylation after oxidative stress exposure as this enzyme is considered to be the main negative regulator of the PI3K pathway. As shown in Figure 4A, Fe^{2+} had no effect on PTEN phosphorylation at all times of incubation. However, in aged-rat synaptosomes (Fig. 4B), PTEN phosphorylation was found to be slightly higher after 5 min of Fe^{2+} exposure and significantly higher after 30 min of exposure. Long-term incubations appear to inhibit PTEN phosphorylation.

Synaptic ERK1/2 Activation after Fe^{2+}-Induced Toxicity

Although studying the PI3K/Akt pathway we also evaluated the effect of Fe^{2+} exposure on the MAPK pathway, in particular on ERK1/2. Figure 5A shows that in adult-rat synaptosomes, Fe^{2+} induced an increase in ERK1/2 phosphorylation after 5 min of incubation, and that this increase was

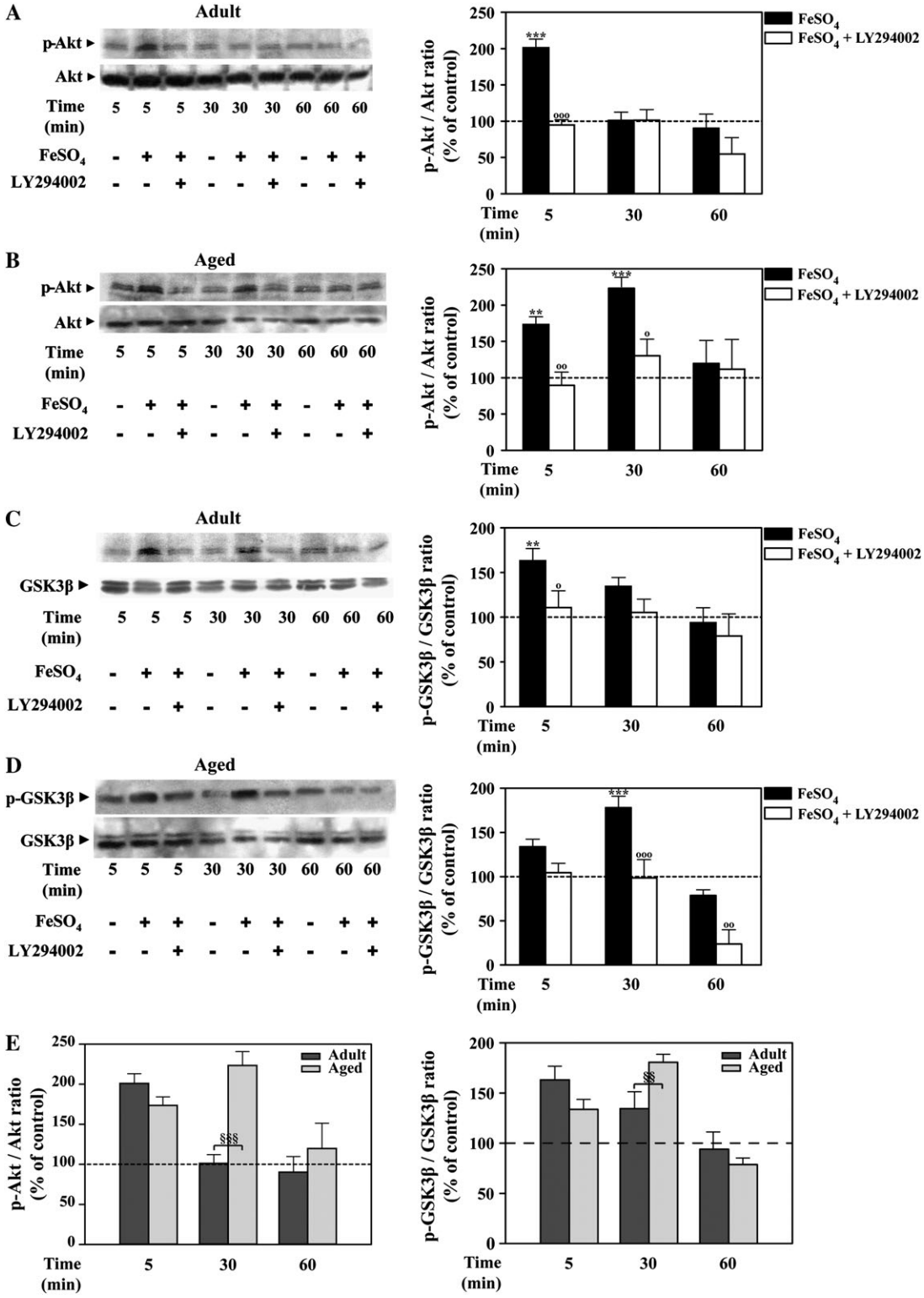

FIG. 3. Effect of Fe^{2+} exposure on PI3K/Akt/GSK3β pathway. (A and B) Western blot analysis of Akt phosphorylation in adult-rat (A) and aged-rat (B) synaptosomes (50 μg protein per lane) exposed to 50μM Fe^{2+} for 5, 30, and 60 min. (C and D) Western blot analysis of GSK3β phosphorylation in adult-rat (C) and aged-rat (D) synaptosomes (50 μg protein per lane) exposed to Fe^{2+} under the same conditions. The Western blot in each case is representative of three different experiments. Bands of proteins were quantified using scanning densitometry, and the data in the graphs on the right represent the ratio between the

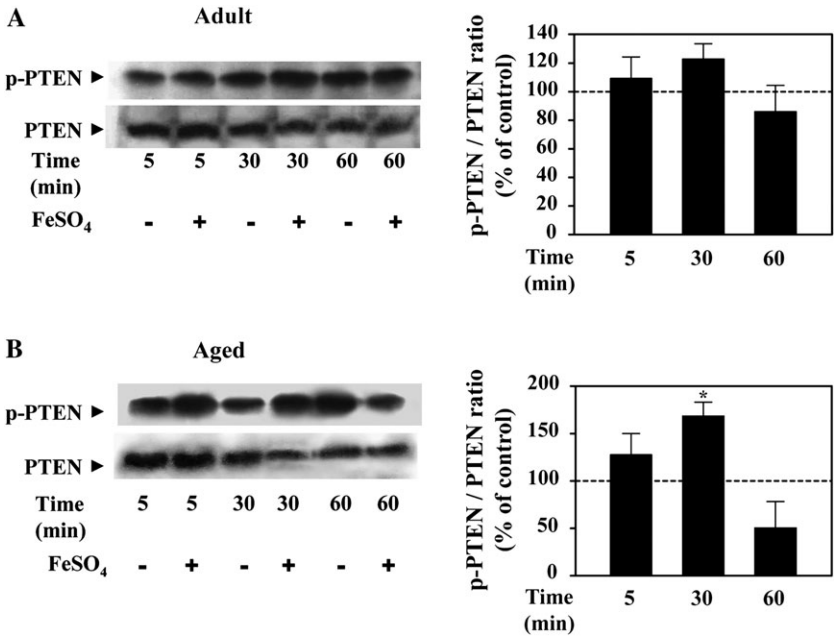

FIG. 4. Effect of Fe^{2+} exposure on PTEN phosphorylation. (A and B) Western blot analysis of PTEN phosphorylation in adult-rat (A) and aged-rat (B) synaptosomes (50 μg protein per lane) exposed to 50μM Fe^{2+} for 5, 30, and 60 min. The Western blot in each case is representative of three different experiments. Bands of proteins were quantified using scanning densitometry, and the data in the graphs on the right represent the ratio between phospho-PTEN and the total level of PTEN, expressed as a percentage of the corresponding control condition (mean ± SD of three different experiments).

totally inhibited by incubating the synaptosomes in the presence of LY294002 prior to metal exposure. This result demonstrates that ERK1/2 are activated downstream of PI3K in adult-rat synaptic endings exposed to metal-induced oxidative stress. The same study was carried out in aged-rat synaptosomes. Fe^{2+} induced a very significant increase in ERK1/2 phosphorylation after a 5-min exposure (Fig. 5B). After 5 min of iron incubation ERK1/2 activation in aged animals was higher (400% with respect to the control) than the activation found in adults (80% with respect to the control). However, ERK1/2 phosphorylation was not abolished by LY294002 which proves that, unlike in adults, ERK1/2 activation in aged-rat synaptic endings is not PI3K dependent.

Participation of Src Tyrosine Kinase in Akt Activation by Oxidative Stress

To investigate whether the tyrosine kinase Src participates in the activation of Akt in cerebral cortex synaptic endings exposed to oxidative stress, we studied the association between Akt and Src. Figure 6A shows that the level of total Akt coimmunoprecipitated with Src was the same in control and Fe^{2+}-exposed adult-rat synaptosomes after a 5-min incubation (the time at which PI3K/Akt activation was verified in adult animals). However, the level of p-Akt associated with Src was much higher for the Fe^{2+}-exposed condition.

Src and Akt association was also studied in aged-rat synaptosomes under the experimental conditions in which Akt is activated (5 and 30 min of Fe^{2+} exposure). As observed in Figure 6B, the level of total Akt coimmunoprecipitated with Src was the same for the control and the oxidative stress-exposed synaptosomes from aged rats after 5 and 30 min of incubation. Surprisingly, the level of p-Akt associated with Src was also the same in both conditions.

Effect of Ca^{2+} on Fe^{2+}-Induced Damage in Synaptic Terminals from Adult and Aged Animals

To determine whether the presence of calcium in the milieu had any effect on iron-induced injury, we carried out the MTT reduction assays in synaptosomes exposed for 5, 30, and 60 min to Fe^{2+} under four different conditions: (1) calcium-free–Locke's buffer + 10μM 1,2-bis-(o-Aminophenoxy)-ethane-N,N,N',N'-tetraacetic acid, tetraacetoxymethyl ester (BAPTA-AM)

phosphorylated state and the total level of each protein, expressed as a percentage of the corresponding control condition (mean ± SD of three different experiments). (E) Comparison between Akt (left panel) and GSK3β (right panel) phosphorylation in adult- and aged-rat synaptic endings. In all cases where LY294002 was used, synaptosomes were preincubated with or without the inhibitor for 10 min before the incubation with the metal ion. ***$p < 0.001$ and **$p < 0.01$ with respect to the control condition; °°°$p < 0.001$, °°$p < 0.01$, and °$p < 0.05$ with respect to ''$FeSO_4$'' condition; $^{§§§}p < 0.001$ and $^{§§}p < 0.01$ when comparing the ''Adult'' versus the ''Aged'' condition.

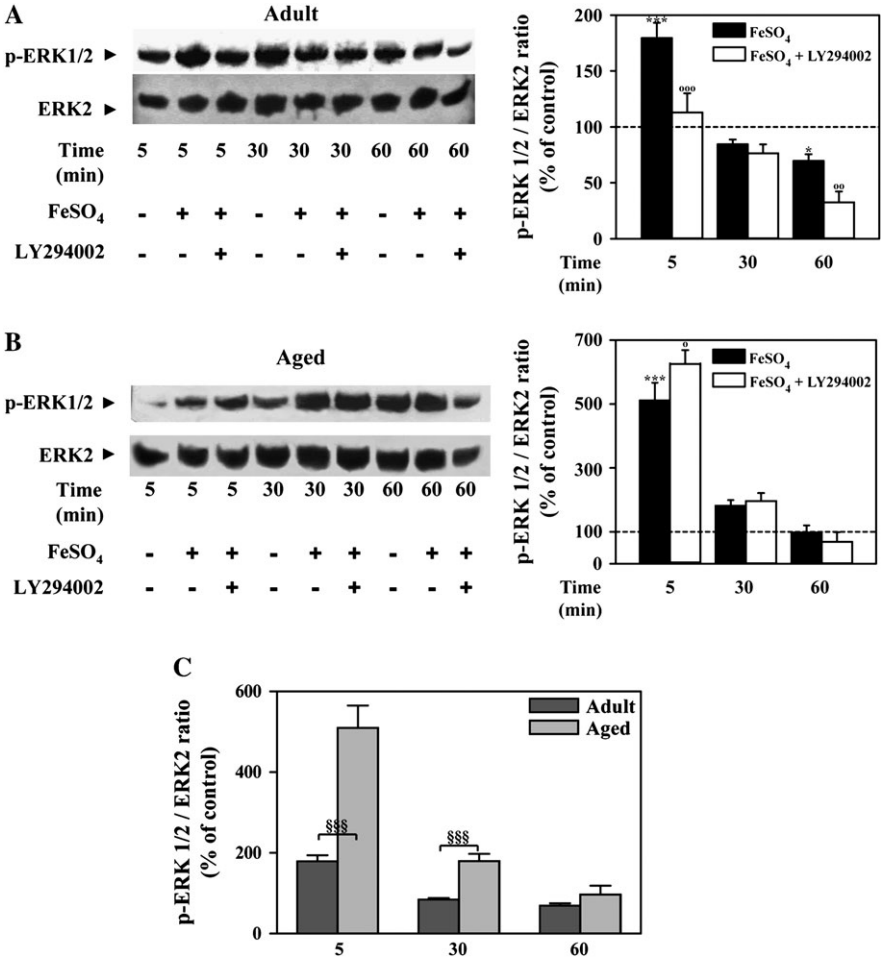

FIG. 5. Effect of Fe^{2+} exposure on ERK1/2 phoshorylation. (A and B) Western blot analysis of ERK1/2 phosphorylation in adult-rat (A) and aged-rat (B) synaptosomes (50 μg protein per lane) exposed to 50μM Fe^{2+} for 5, 30, and 60 min. (C) Comparison of ERK1/2 phosphorylated levels after Fe^{2+} exposure in synaptosomes obtained from adult and aged rats. The Western blot in each case is representative of three different experiments. Bands of proteins were quantified using scanning densitometry, and phospho-ERK1/2 levels were normalized to total ERK2 levels and expressed as a percentage of the corresponding control condition (mean ± SD of three different experiments).

(intracellular Ca^{2+} chelator); (2) calcium free-Locke's buffer; (3) normal calcium-Locke's buffer; (4) normal calcium-Locke's buffer + 10μM A23187 (a calcium ionophore). As can be seen in Figure 7A, the only condition to show a significant decrease in mitochondrial viability with respect to the control after 5 min of incubation in the presence of Fe^{2+} was condition 3 (normal calcium-Locke's buffer). Condition 4 (normal calcium-Locke's buffer + 10μM A23187) showed the greatest damage, though this was due not to Fe^{2+} but to excess Ca^{2+} caused by the ionophore. Figure 7B shows that mitochondrial viability was diminished with respect to the controls in all the Fe^{2+}-exposed conditions after 30 min. Surprisingly, Figure 7C shows that after 60 min of incubation it was condition 3 (normal calcium-Locke's buffer) that presented the least damage in the presence of Fe^{2+}.

When a similar analysis was performed on synaptosomes from aged rats, the same results were observed as those found in adults, the only difference being that the levels of damage were higher for synaptosomes from aged rats (Figs. 7D–F).

Effect of Fe^{2+} Exposure on Akt Phosphorylation. Calcium Dependence

After determining that the PI3K/Akt pathway was activated by Fe^{2+} exposure, we wondered whether this activation was dependent on the presence of Ca^{2+}. To answer this question Akt phosphorylation was assessed by Western blot in synaptosomes exposed for 5, 30, and 60 min to Fe^{2+} under the four above-mentioned conditions. As can be seen in Figure 8A, a 5-min exposure to the metal ion induced an increase in Akt phosphorylation only under condition 3 (normal calcium-Locke's buffer). Figures 8B and 8C show that 30- and 60-min exposures did not activate Akt in adult-rat synaptosomes. Coincidently, when Ca^{2+}-requirement for Akt activation was tested in aged-rat synaptosomes, it was found that Akt was

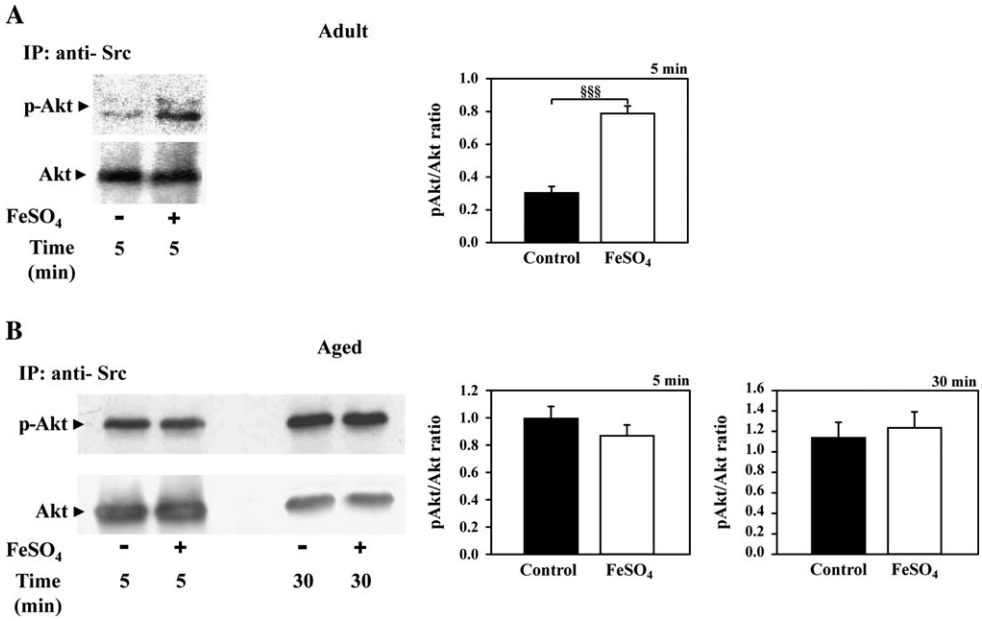

FIG. 6. Akt-Src interaction. (A) Immunoprecipitations of Src were performed after exposing adult-rat synaptosomes (2 mg protein/ml) to 50μM Fe^{2+} for 5 min. Western blot analyses of the IPs were carried out by using the antibodies detailed in the figure. The Western blot shown in each case is representative of three different experiments. Bands of proteins were quantified using scanning densitometry, and p-Akt/Akt ratio is shown in the bar graph on the right. (B) The same immunoprecipitations were performed in synaptic endings from aged rats (2 mg protein/ml) exposed to 50μM Fe^{2+} for 5 and 30 min. The antibodies used for these analyses were the same as those used in *A*. Each Western blot is representative of three different experiments. Bands of proteins were quantified using scanning densitometry, and p-Akt/Akt ratio is shown in the bar graphs on the right.

activated after 5 min of incubation in the presence of Fe^{2+} only under condition 3 (normal calcium-Locke's buffer) (Fig. 9A). However, Akt was also activated after a 30-min iron exposure, both in the absence (conditions 1 and 2) and presence (condition 3) of Ca^{2+}. There was no activation in the presence of excess Ca^{2+} (condition 4) (Figs. 9B and 9C).

DISCUSSION

The increased lifespan of today has had a marked impact on the appearance of chronic and degenerative diseases in elderly people. Over the years, metalloneurobiology has become extremely important for establishing the role of transition metals in neuronal degeneration. It is well documented that the increase in Fe^{2+} levels in the affected cerebral areas of AD patients and the oxidative stress induced by this metal play a key role in the pathogenesis of several neurodegenerative diseases (Berg and Youdim, 2006). It has been observed that this metal ion progressively accumulates in the brain both during normal aging and also in neurodegenerative processes (Bartzokis *et al*., 2004). However, iron accumulation in AD occurs without the concomitant increase in ferritin normally observed in aging (Connor *et al*., 1992). This event generates an increase in the metal levels and, therefore, in the risk of oxidative stress (Thompson *et al*., 2003). Another important hallmark of neurodegeneration is synaptic loss. Synaptic loss and the impairment of synaptic signaling pathways are early events in neurodegenerative processes triggered by oxidative stress. However, the mechanisms underlying synaptic death during aging and neurodegeneration are poorly understood.

In this paper, we characterize the iron-induced neurotoxicity in synaptic endings from adult and aged rats and the state of signaling pathways involved in neuronal survival and death such as PI3K/Akt/GSK3β and ERK1/2.

MTT reduction assay and LDH leakage, as a measure of mitochondrial function and membrane integrity, show that synaptic endings from aged animals are more susceptible to iron exposure than adult ones. These results coincide with numerous studies demonstrating the impairment of synaptic functions as an outcome of aging, for instance changes in synaptic plasma membrane fluidity, in calcium homeostasis, and in intracellular signaling (Calderini *et al*., 1983; Foster and Kumar, 2002). Several reports have suggested that the impairment of mitochondrial function as a consequence of oxidative stress is the main contributor to age-related cerebral alterations (Floyd and Hensley, 2002; Navarro and Boveris, 2004). In this sense, cerebral mitochondria of aged people are particularly vulnerable to lipid peroxidation due to their high oxygen consumption and high content in polyunsaturated fatty acids, their poor antioxidant defense, and their high content in cerebral transition metals. Akt was shown to be activated only after a short insult in adults. However, in aged animals this kinase was activated not only after a brief exposure to the insult

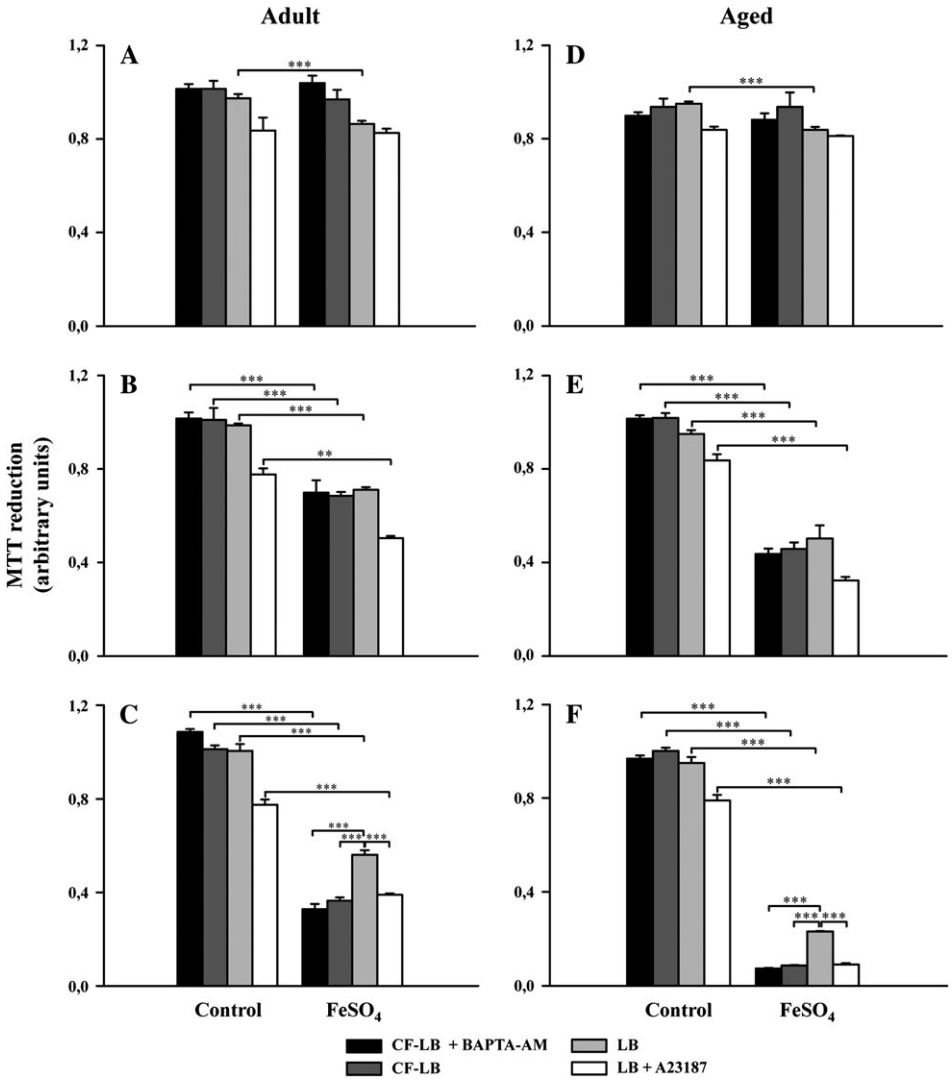

FIG. 7. MTT reduction assay: calcium dependence. Adult-rat (A, B, and C) and aged-rat (D, E, and F) synaptosomes were resuspended (2 mg protein/ml) in four different conditions: calcium-free–Locke's buffer + 10μM BAPTA-AM (CF-LB + BAPTA-AM), calcium-free–Locke's buffer (CF-LB), normal calcium-Locke's buffer (LB), normal calcium-Locke's buffer + 10μM A23187 (LB + A23187), and incubated in the presence of 50μM Fe^{2+} for different periods of time 5 (A and D), 30 (B and E), and 60 (C and F) min. Results are expressed as arbitrary units and represent the mean ± SD, $n = 3–6$. ***$p < 0.001$ and **$p < 0.01$.

but also after 30 min of iron exposure. The sustained activation of Akt triggered by free iron in aged animals could be another molecular marker of age-related susceptibility as it was observed in MTT and LDH assays. In this connection, several studies have demonstrated that Akt can be differentially activated in control and aged neurons (Nie *et al.*, 2009; Song *et al.*, 2007). One of the best-known Akt substrates, GSK3β, is involved in numerous cellular functions such as metabolism, survival, gene expression, and cytoskeletal dynamics (Grimes and Jope, 2001). Its activity is inhibited by phosphorylation in a Ser9 residue. We demonstrated that iron-induced GSK3β phosphorylation and that this inhibition was a PI3K-dependent event in adult animals. In the same way, synaptosomes from aged animals showed that the increase in GSK3β phosphorylation was temporally coincident with Akt phosphorylation and also dependent on PI3K activation. We demonstrate here that the whole pathway, PI3K/Akt/GSK3β, is activated in synaptic endings from both adult and aged rats exposed to free iron-induced oxidative injury. However, the inactivation of GSK3β by Akt is most pronounced in aged animals. Dysregulation of GSK3β activity is believed to play a key role in the pathogenesis of central nervous system chronic disorders such as AD, bipolar disorder, and Huntington's disease (Songin *et al.*, 2007; Takashima, 2009). In this aspect, GSK3β inhibitors have been postulated as therapeutic tools for these diseases (Rametti *et al.*, 2008). Interestingly, pathophysiological and pharmacological regulation of GSK3β is affected by an amplification mechanism: a sustained inhibition or

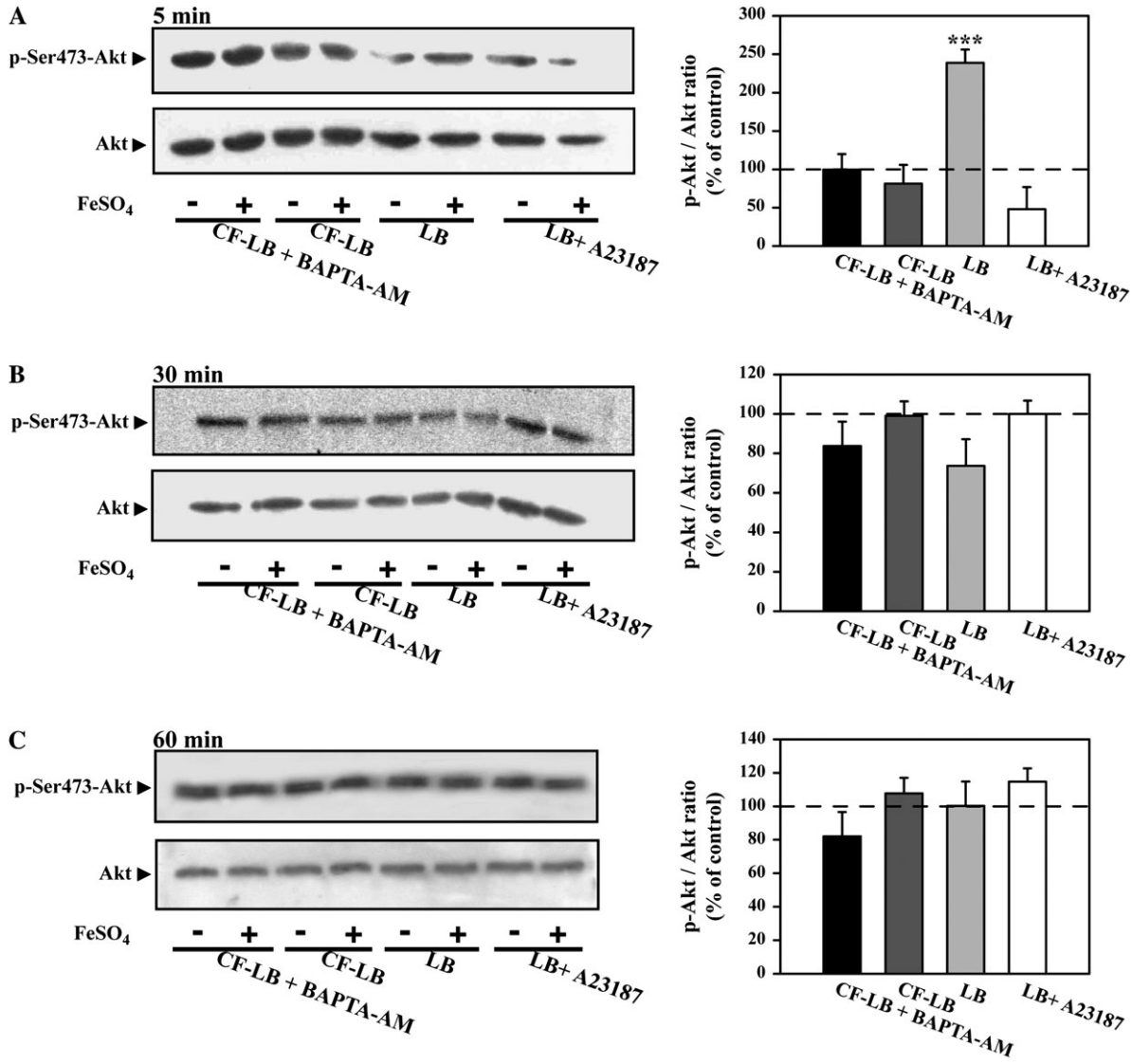

FIG. 8. Akt activation in adult synaptosomes: calcium dependence. Adult-rat synaptosomes were resuspended under the same set of four different conditions described in Figure 7 and incubated in the presence of 50μM Fe^{2+} for the same times as those described there. Samples were loaded onto 10% SDS-PAGE gels (50 μg synaptosomal protein per lane) and Akt phosphorylation was evaluated by Western blot analysis. Each Western blot is representative of three different experiments. Bands of proteins were quantified using scanning densitometry. p-Akt/Akt ratio are shown in the right panels, expressed as percentage of control.

activation of GSK3β might persist after cessation of the initial trigger (Meijer *et al*., 2004). The increased persistence of Akt activation and GSK3β inhibition in aged animals could be due to an augmented susceptibility to iron-induced neurotoxicity.

ERK1/2 activation has been reported to be involved both in neuronal survival and cellular death, and it is well known that PI3K can exert either a stimulatory or an inhibitory effect on ERK1/2 depending on the identity and the power of the extracellular stimuli applied (Duckworth and Cantley, 1997; Wennstrom and Downward, 1999). Furthermore, it has been reported that presynaptic ERK signaling modulates neurotransmitter release. In adult animals, ERK1/2 activation occurred after a brief exposure to Fe^{2+} and was PI3K dependent. These findings are in agreement with those reported by Crossthwaite *et al*. (2002), where PI3K positively contributes to ERK1/2 activation in cortical neurons exposed to oxidative stress induced by hydrogen peroxide. In synaptosomes from aged animals, ERK1/2 activation also occurred after short time of incubation in the presence of the metal ion (and still remained activated to a lesser extent after 30 min of incubation) but was not PI3K dependent. Many changes in ERK1/2 activities have been reported to occur in cerebral cortex during aging, such changes not being due to different protein levels (Zhen *et al*., 1999). This cascade has been considered as an integrator in the signaling of learning and memory processes (Simonyi *et al*.,

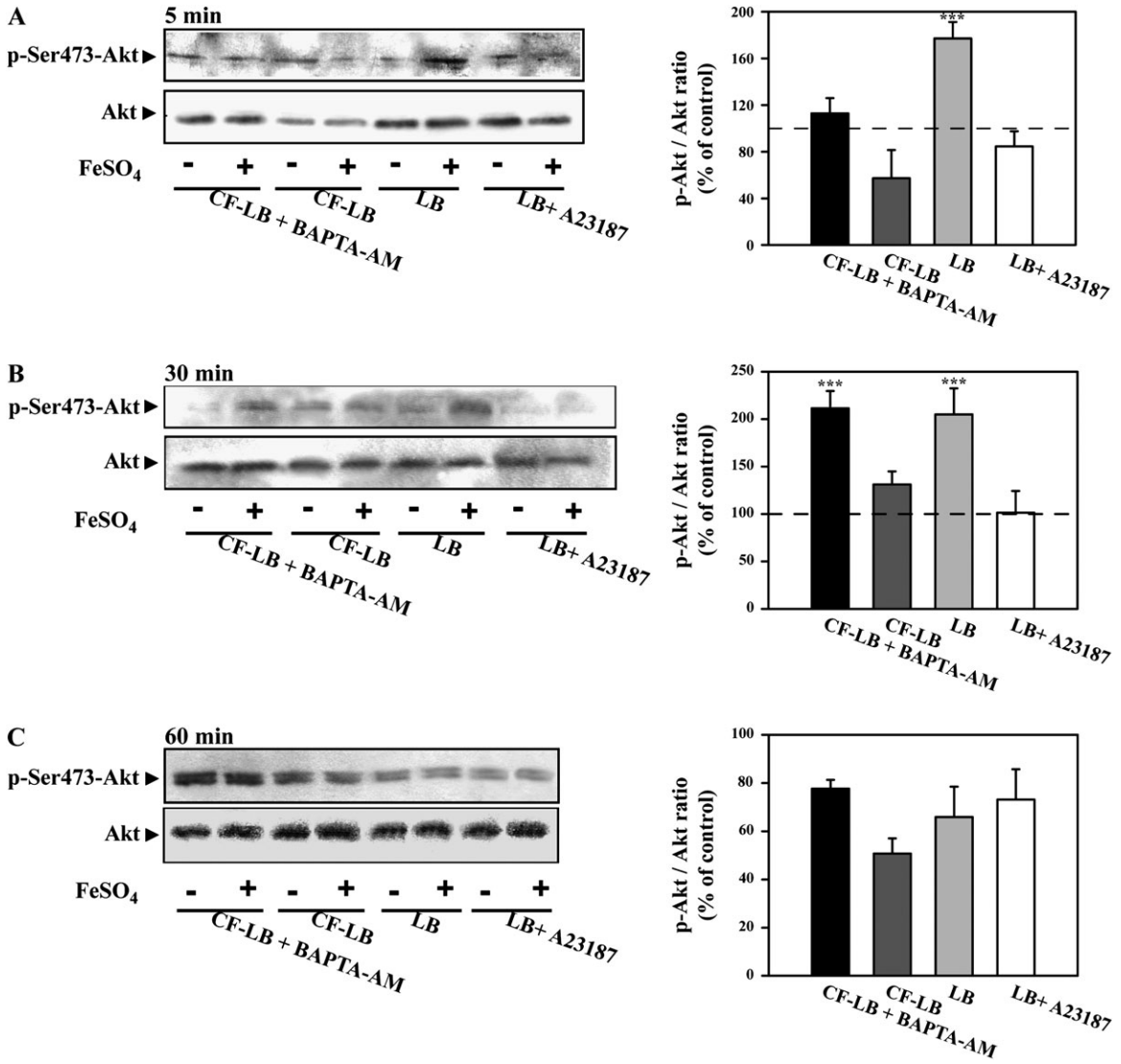

FIG. 9. Akt activation in aged synaptosomes: calcium dependence. Aged-rat synaptosomes were resuspended under the same set of four different conditions described in Figure 7 and incubated in the presence of 50μM Fe^{2+} for the same times as those described there. Akt phosphorylation was evaluated by Western blot analysis (50 μg synaptosomal protein per lane). Each Western blot is representative of three different experiments. Bands of proteins were quantified using scanning densitometry. p-Akt/Akt ratio are shown in the right panels, expressed as percentage of control.

2003), and age-related changes in ERK1/2 activation are thought to be dependent on different activation.

Several members of the Src family, which include Src, Fyn, and Lyn, are expressed at high levels in the adult brain, and both Src and Fyn localize to postsynaptic densities (Boxall and Lancaster, 1998). This family of nonreceptor tyrosine kinases are key regulators of synaptogenesis, memory improvement, and neurorepair. It has been also proposed that Src is the kinase responsible for both Akt recruitment and tyrosine-phosphorylation (Jiang and Qiu, 2003). More specifically, it has been proved that Src participates in the regulation of hippocampal synaptic activity during learning and memory. Our results show that there is a strong association between Akt and Src in the synaptic endings and that the level of activated Akt associated with Src was notably higher in the metal-exposed condition in adult synaptic endings. However, in synaptosomes from aged animals, the association Akt-Src was found to differ from that observed in adults: activated Akt levels associated with Src were equivalent in the control condition and in metal-treated synaptosomes. The differential association between Src and activated Akt observed in aged animals could indicate a misregulation in the mechanism of Akt modulation.

Under physiological conditions, intracellular calcium level is tightly controlled, and relatively small changes in intracellular calcium content might gradually and cumulatively

result in neuronal deterioration, and might eventually lead to cell degeneration. The role of free calcium in neuronal death induced by oxidative stress has been well documented (Mattson, 2007; Ray *et al*., 2000; Wojda *et al*., 2008). We noticed that after a brief exposure (5 min) to the oxidative insult, the only condition that showed greater mitochondrial damage than its corresponding control was that where synaptosomes were incubated in the presence of both intra- and extrasynaptosomal calcium (i.e., Locke's buffer). Intermediate- and long-term incubations (30 and 60 min, respectively) with Fe^{2+} impaired mitochondrial function independently of the presence or the absence of calcium. Surprisingly, long-term Fe^{2+}-incubations in Locke's buffer showed less damage than the other Fe^{2+}-containing calcium conditions. Our results suggest that calcium participates in the early events of oxidative injury in synaptosomes but that when incubation times are longer, absence or excess of this cation appears to be more deleterious to the synaptic endings than the damage induced by Fe^{2+} itself. Although Ca^{2+} dysregulation is a hallmark in neurodegeneration processes, the exact mechanism by which Ca^{2+} ions actually mediate excitotoxicity is not clear. One of the most accepted hypotheses suggests that Ca^{2+}-dependent neurotoxicity occurs following the activation of distinct signaling cascades downstream from key points of Ca^{2+} entry at synapses. Another hypothesis is that calcium influx participates in the activation of calpains. Calpains are heavily concentrated in the synaptic endings and they actively participate in synaptic function (Liu *et al*., 2008; Nixon *et al*., 1994). Deleterious effect observed in our experimental model at long incubation time could involve the activation of calpains. However, additional studies are needed in order to clarify the exact role of calpains in iron-induced neurotoxicity.

We have recently determined that phosphatidylcholine (PC) breakdown is activated in synaptic endings exposed to iron-induced oxidative injury. However, PC-derived signaling was not affected in aged animals exposed to the oxidative insult (Mateos *et al*., 2008). In this work we show that synaptic endings from aged animals are more susceptible to the oxidative injury and we also describe a differential regulation of PI3K signaling than that observed in adult animals. The role of synaptic PI3K in mediating the effects of physical stress on hippocampal plasticity has been confirmed (Kelly and Lynch, 2000). There is also evidence pointing to the local action of signaling pathways in the preservation of mitochondrial function in nerve terminals through events that must be necessarily gene-transcription independent (Guo and Mattson, 2000). The results presented in this paper clearly demonstrate that the synaptic signaling triggered by free iron–induced oxidative stress differ in adult and aged animals. The available data in the literature together with our results suggest that in more susceptible, such as aged, synaptic endings, oxidative stress–triggered PI3K/Akt activation could have a different goal than that pursued in adult synaptic terminals.

FUNDING

Universidad Nacional del Sur (24/B137); Agencia Nacional de Promoción Científica (FONCYT, PICT 01-14527) to N.M.G.; Agencia Nacional de Promoción Científica (FONCYT, PICT 15-20352) to G.A.S.; Consejo Nacional de Investigaciones Científicas y Técnicas (CONICET, PIP 5539) to N.M.G and G.A.S.

ACKNOWLEDGMENTS

Dr Norma M. Giusto and Dr Gabriela A. Salvador are research members of the CONICET. Romina M. Uranga is a research fellow of the CONICET. Authors thank Dr Silvia Antollini for her helpful assistance in the fluorimetric measurements of ROS levels.

REFERENCES

Anselmo, A. N., and Cobb, M. H. (2004). Protein kinase function and glutathionylation. *Biochem. J.* **381**(Pt 3), e1–e2.

Bartzokis, G., Tishler, T. A., Shin, I. S., Lu, P. H., and Cummings, J. L. (2004). Brain ferritin iron as a risk factor for age at onset in neurodegenerative diseases. *Ann. N. Y. Acad. Sci.* **1012,** 224–236.

Berg, D., and Youdim, M. B. (2006). Role of iron in neurodegenerative disorders. *Top. Magn. Reson. Imaging* **17,** 5–17.

Boxall, A. R., and Lancaster, B. (1998). Tyrosine kinases and synaptic transmission. *Eur. J. Neurosci.* **10,** 2–7.

Calderini, G., Bonetti, A. C., Battistella, A., Crews, F. T., and Toffano, G. (1983). Biochemical changes of rat brain membranes with aging. *Neurochem. Res.* **8,** 483–492.

Coelho, C. M., and Leevers, S. J. (2000). Do growth and cell division rates determine cell size in multicellular organisms? *J. Cell. Sci.* **113**(Pt 17), 2927–2934.

Connor, J. R., Snyder, B. S., Beard, J. L., Fine, R. E., and Mufson, E. J. (1992). Regional distribution of iron and iron-regulatory proteins in the brain in aging and Alzheimer's disease. *J. Neurosci. Res.* **31,** 327–335.

Cotman, C. W. (1974). Isolation of synaptosomal and synaptic plasma membrane fractions. *Methods Enzymol.* **31**(Pt A), 445–452.

Crossthwaite, A. J., Hasan, S., and Williams, R. J. (2002). Hydrogen peroxide-mediated phosphorylation of ERK1/2, Akt/PKB and JNK in cortical neurones: Dependence on Ca(2+) and PI3-kinase. *J. Neurochem.* **80,** 24–35.

Datta, S. R., Dudek, H., Tao, X., Masters, S., Fu, H., Gotoh, Y., and Greenberg, M. E. (1997). Akt phosphorylation of BAD couples survival signals to the cell-intrinsic death machinery. *Cell* **91,** 231–241.

Duckworth, B. C., and Cantley, L. C. (1997). Conditional inhibition of the mitogen-activated protein kinase cascade by wortmannin. Dependence on signal strength. *J. Biol. Chem.* **272,** 27665–27670.

Floyd, R. A., and Hensley, K. (2002). Oxidative stress in brain aging. Implications for therapeutics of neurodegenerative diseases. *Neurobiol. Aging* **23,** 795–807.

Foster, T. C., and Kumar, A. (2002). Calcium dysregulation in the aging brain. *Neuroscientist* **8,** 297–301.

Fry, M. J. (2001). Phosphoinositide 3-kinase signalling in breast cancer: How big a role might it play? *Breast Cancer Res.* **3,** 304–312.

Grimes, C. A., and Jope, R. S. (2001). The multifaceted roles of glycogen synthase kinase 3beta in cellular signaling. *Prog. Neurobiol.* **65,** 391–426.

Guo, Z. H., and Mattson, M. P. (2000). Neurotrophic factors protect cortical synaptic terminals against amyloid and oxidative stress-induced impairment of glucose transport, glutamate transport and mitochondrial function. *Cereb. Cortex* **10,** 50–57.

Jacobson, M. D., Burne, J. F., and Raff, M. C. (1994). Programmed cell death and Bcl-2 protection in the absence of a nucleus. *EMBO J.* **13,** 1899–1910.

Jiang, T., and Qiu, Y. (2003). Interaction between Src and a C-terminal proline-rich motif of Akt is required for Akt activation. *J. Biol. Chem.* **278,** 15789–15793.

Katso, R., Okkenhaug, K., Ahmadi, K., White, S., Timms, J., and Waterfield, M. D. (2001). Cellular function of phosphoinositide 3-kinases: Implications for development, homeostasis, and cancer. *Annu. Rev. Cell Dev. Biol.* **17,** 615–675.

Kauffmann-Zeh, A., Rodriguez-Viciana, P., Ulrich, E., Gilbert, C., Coffer, P., Downward, J., and Evan, G. (1997). Suppression of c-Myc-induced apoptosis by Ras signalling through PI(3)K and PKB. *Nature* **385,** 544–548.

Keller, J. N., Mark, R. J., Bruce, A. J., Blanc, E., Rothstein, J. D., Uchida, K., Waeg, G., and Mattson, M. P. (1997). 4-Hydroxynonenal, an aldehydic product of membrane lipid peroxidation, impairs glutamate transport and mitochondrial function in synaptosomes. *Neuroscience* **80,** 685–696.

Kelly, A., and Lynch, M. A. (2000). Long-term potentiation in dentate gyrus of the rat is inhibited by the phosphoinositide 3-kinase inhibitor, wortmannin. *Neuropharmacology* **39,** 643–651.

Kenyon, C. (2005). The plasticity of aging: Insights from long-lived mutants. *Cell* **120,** 449–460.

Laemmli, U. K. (1970). Cleavage of structural proteins during the assembly of the head of bacteriophage T4. *Nature* **227,** 680–685.

Liu, J., Liu, M. C., and Wang, K. K. (2008). Calpain in the CNS: From synaptic function to neurotoxicity. *Sci. Signal.* **1**(14), re1.

Lowry, O. H., Rosebrough, N. J., Farr, A. L., and Randall, R. J. (1951). Protein measurement with the Folin phenol reagent. *J. Biol. Chem.* **193,** 265–275.

Mateos, M. V., Uranga, R. M., Salvador, G. A., and Giusto, N. M. (2008). Activation of phosphatidylcholine signalling during oxidative stress in synaptic endings. *Neurochem. Int.* **53,** 199–206.

Mattson, M. P. (2007). Calcium and neurodegeneration. *Aging Cell* **6,** 337–350.

Meijer, L., Flajolet, M., and Greengard, P. (2004). Pharmacological inhibitors of glycogen synthase kinase 3. *Trends Pharmacol. Sci.* **25,** 471–480.

Navarro, A., and Boveris, A. (2004). Rat brain and liver mitochondria develop oxidative stress and lose enzymatic activities on aging. *Am. J. Physiol. Regul. Integr. Comp. Physiol.* **287,** R1244–R1249.

Nie, K., Yu, J. C., Fu, Y., Cheng, H. Y., Chen, F. Y., Qu, Y., and Han, J. X. (2009). Age-related decrease in constructive activation of Akt/PKB in SAMP10 hippocampus. *Biochem. Biophys. Res. Commun.* **378,** 103–107.

Niwa, K., Inanami, O., Ohta, T., Ito, S., Karino, T., and Kuwabara, M. (2001). p38 MAPK and Ca2+ contribute to hydrogen peroxide-induced increase of permeability in vascular endothelial cells but ERK does not. *Free Radic. Res.* **35,** 519–527.

Nixon, R. A., Saito, K. I., Grynspan, F., Griffin, W. R., Katayama, S., Honda, T., Mohan, P. S., Shea, T. B., and Beermann, M. (1994). Calcium-activated neutral proteinase (calpain) system in aging and Alzheimer's disease. *Ann. N. Y. Acad. Sci.* **747,** 77–91.

Nunomura, A., Perry, G., Aliev, G., Hirai, K., Takeda, A., Balraj, E. K., Jones, P. K., Ghanbari, H., Wataya, T., Shimohama, S., *et al.* (2001). Oxidative damage is the earliest event in Alzheimer disease. *J. Neuropathol. Exp. Neurol.* **60,** 759–767.

Rametti, A., Esclaire, F., Yardin, C., Cogné, N., and Terro, F. (2008). Lithium down-regulates tau in cultured cortical neurons: A possible mechanism of neuroprotection. *Neurosci. Lett.* **434,** 93–98.

Ray, S. K., Fidan, M., Nowak, M. W., Wilford, G. G., Hogan, E. L., and Banik, N. L. (2000). Oxidative stress and Ca2+ influx upregulate calpain and induce apoptosis in PC12 cells. *Brain Res.* **852,** 326–334.

Simonyi, A., Murch, K., and Sun, G. Y. (2003). Extracellular signal-regulated kinase 2 mRNA expression in the rat brain during aging. *Neurochem. Res.* **28,** 1375–1378.

Song, G. Y., Kang, J. S., Lee, S. Y., and Myung, C. S. (2007). Region-specific reduction of Gbeta4 expression and induction of the phosphorylation of PKB/Akt and ERK1/2 by aging in rat brain. *Pharmacol. Res.* **56,** 295–302.

Songin, M., Jeśko, H., Czapski, G., Adamczyk, A., and Strosznajder, R. P. (2007). GSK-3beta and oxidative stress in aged brain. Role of poly(ADP-ribose) polymerase-1. *Folia Neuropathol.* **45,** 220–229.

Sun, W., Kesavan, K., Schaefer, B. C., Garrington, T. P., Ware, M., Johnson, N. L., Gelfand, E. W., and Johnson, G. L. (2001). MEKK2 associates with the adapter protein Lad/RIBP and regulates the MEK5-BMK1/ERK5 pathway. *J. Biol. Chem.* **276,** 5093–5100.

Takashima, A. (2009). Drug development targeting the glycogen synthase kinase-3beta (GSK-3beta)-mediated signal transduction pathway: Role of GSK-3beta in adult brain. *J. Pharmacol. Sci.* **109,** 174–178.

Thompson, K., Menzies, S., Muckenthaler, M., Torti, F. M., Wood, T., Torti, S. V., Hentze, M. W., Beard, J., and Connor, J. (2003). Mouse brains deficient in H-ferritin have normal iron concentration but a protein profile of iron deficiency and increased evidence of oxidative stress. *J. Neurosci. Res.* **71,** 46–63.

Uranga, R. M., Mateos, M. V., Giusto, N. M., and Salvador, G. A. (2007). Activation of phosphoinositide-3 kinase/Akt pathway by FeSO4 in rat cerebral cortex synaptic endings. *J. Neurosci. Res.* **85,** 2924–2932.

Wennstrom, S., and Downward, J. (1999). Role of phosphoinositide 3-kinase in activation of ras and mitogen-activated protein kinase by epidermal growth factor. *Mol. Cell Biol.* **19,** 4279–4288.

Wojda, U., Salinska, E., and Kuznicki, J. (2008). Calcium ions in neuronal degeneration. *IUBMB. Life* **60,** 575–590.

Zago, M. P., Mackenzie, G. G., Adamo, A. M., Keen, C. L., and Oteiza, P. I. (2005). Differential modulation of MAP kinases by zinc deficiency in IMR-32 cells: Role of H(2)O(2). *Antioxid. Redox. Signal.* **7,** 1773–1782.

Zhen, X., Uryu, K., Cai, G., Johnson, G. P., and Friedman, E. (1999). Age-associated impairment in brain MAPK signal pathways and the effect of caloric restriction in Fischer 344 rats. *J. Gerontol. A Biol. Sci. Med. Sci.* **54,** B539–B548.

Zhu, X., Raina, A. K., Lee, H. G., Casadesus, G., Smith, M. A., and Perry, G. (2004). Oxidative stress signalling in Alzheimer's disease. *Brain Res.* **1000,** 32–39.